Inhibition of pluripotent stem cell-derived teratoma formation by small molecules

Mi-Ok Lee[a,1], Sung Hwan Moon[b], Ho-Chang Jeong[a], Ji-Yeon Yi[c], Tae-Hee Lee[c], Sung Han Shim[b], Yong-Hee Rhee[d], Sang-Hun Lee[d], Seok-Jeong Oh[e], Moo-Yeol Lee[e], Min-Joon Han[f], Yee Sook Cho[g], Hyung-Min Chung[h], Kwang-Soo Kim[f,2], and Hyuk-Jin Cha[a,2]

[a]Department of Life Sciences, College of Natural Sciences, Sogang University, Seoul 121-742, Korea; [b]Department of Biomedical Science, College of Life Science, CHA University, Pochon-si Gyeonggi-do 487-010, Korea; [c]Laboratory of Cancer and Stem Cell Biology, Plant Engineering Institute, Sejong University, Seoul 143-747, Korea; [d]Department of Biochemistry and Molecular Biology, College of Medicine, Hanyang University, Seoul 133-791, Korea; [e]College of Pharmacy, Dongguk University, Seoul 100-715, Korea; [f]Molecular Neurobiology Laboratory, Department of Psychiatry, McLean Hospital, Harvard Medical School, Belmont, MA 02478; [g]Stem Cell Research Center, Korea Research Institute of Bioscience and Biotechnology, Daejeon 305-806, Korea; and [h]Department of Stem Cell Biology, Konkuk University School of Medicine, Seoul 143-701, Korea

Edited* by Gregory A. Petsko, Brandeis University, Waltham, MA, and approved July 5, 2013 (received for review February 26, 2013)

The future of safe cell-based therapy rests on overcoming teratoma/tumor formation, in particular when using human pluripotent stem cells (hPSCs), such as human embryonic stem cells (hESCs) and human induced pluripotent stem cells (hiPSCs). Because the presence of a few remaining undifferentiated hPSCs can cause undesirable teratomas after transplantation, complete removal of these cells with no/minimal damage to differentiated cells is a prerequisite for clinical application of hPSC-based therapy. Having identified a unique hESC signature of pro- and antiapoptotic gene expression profile, we hypothesized that targeting hPSC-specific antiapoptotic factor(s) (i.e., survivin or Bcl10) represents an efficient strategy to selectively eliminate pluripotent cells with teratoma potential. Here we report the successful identification of small molecules that can effectively inhibit these antiapoptotic factors, leading to selective and efficient removal of pluripotent stem cells through apoptotic cell death. In particular, a single treatment of hESC-derived mixed population with chemical inhibitors of survivin (e.g., quercetin or YM155) induced selective and complete cell death of undifferentiated hPSCs. In contrast, differentiated cell types (e.g., dopamine neurons and smooth-muscle cells) derived from hPSCs survived well and maintained their functionality. We found that quercetin-induced selective cell death is caused by mitochondrial accumulation of p53 and is sufficient to prevent teratoma formation after transplantation of hESC- or hiPSC-derived cells. Taken together, these results provide the "proof of concept" that small-molecule targeting of hPSC-specific antiapoptotic pathway(s) is a viable strategy to prevent tumor formation by selectively eliminating remaining undifferentiated pluripotent cells for safe hPSC-based therapy.

The unique properties of human pluripotent stem cells (hPSCs) such as human embryonic stem cells (hESCs) and human induced pluripotent stem cells (hiPSC) [i.e., indefinite self-renewal in vitro while maintaining their ability to differentiate into all cell types of the body upon exposure to relevant differentiation signals (1–3)] make them the best potential cell source for cell-based regenerative therapy and/or personalized medicine (4). Thus, enormous efforts have been undertaken to establish hESC- and hiPSC-based therapies for a variety of degenerative diseases (4–7). However, there are major technical and scientific obstacles remaining to be overcome before hPSC-based cell therapy becomes a realistic therapeutic modality. Most of all, it is of utmost importance to avoid possible teratoma/tumor formation that can arise from any remaining undifferentiated pluripotent stem cells present in the differentiated cell mixture (8). Indeed, a systematic transplantation study demonstrated that the teratoma-forming propensity of various mouse iPSC-derived neurospheres correlated with the persistence of residual undifferentiated cells (9). Because hESCs and hiPSCs also exhibit marked variations in differentiation efficiencies (and remaining undifferentiated cells) (10–13), it is critical to remove all residual hiPSCs with teratoma potential before their clinical application. Despite numerous attempts at blocking teratoma formation, including introduction of suicide genes (14) or selecting the desired cell type (15), immunodepletion (16), or introducing cytotoxic antibody (17), a clinically viable strategy to eliminate teratoma formation remains to be developed (8, 18).

Notably, ESCs are highly susceptible to apoptotic stimuli (19, 20), which seems to be related to their relatively low frequency of spontaneous mutation (21). Because early embryonic cells contribute to all tissue types during later developmental stages, it is crucial to minimize the risk of potential genetic alterations in early embryonic cells, which would explain their hypersensitivity to apoptosis in response to genotoxic and environmental stress (19, 22, 23). Thus, it is likely that hPSCs have unique profiles and/or apoptotic mechanisms that are significantly different from those of differentiated cell types. In line with this, previous studies demonstrated that a distinct mitochondrial p53 function regulates apoptotic signals in ESCs (19, 22). The mitochondrial localization of p53 was suggested to be the result from unique posttranslational modification (PTM) of undifferentiated hESCs under genotoxic stress (19). Furthermore, a recent study showed that a constitutively active form of BCL2-associated X (*BAX*) protein is present in the Golgi complex of hESCs and is translocated to the mitochondria under DNA damage stress, leading to rapid apoptotic response (24). Taking advantage of the high susceptibility to DNA damage, genotoxic agents were recently suggested to lower teratoma risk of PSCs (25).

We speculated that deeper understanding of the expression profiles of pro- and antiapoptotic genes in hESCs would provide

Significance

We found that quercetin/YM155-induced selective cell death is sufficient to completely inhibit teratoma formation after transplantation of human pluripotent stem cell (hPSC)-derived cells. These data provide the first "proof of concept" that small-molecule targeting of hPSC-specific antiapoptotic pathway(s) is a viable strategy to prevent tumor formation by selectively eliminating remaining undifferentiated pluripotent cells for safe hPSC-based therapy.

Author contributions: M.-O.L., K.-S.K., and H.-J.C. designed research; M.-O.L., S.H.M., H.-C.J., J.-Y.Y., T.-H.L., S.H.S., Y.-H.R., S.-J.O., and M.-J.H. performed research; Y.S.C. contributed new reagents/analytic tools; M.-O.L., S.-H.L., M.-Y.L., H.-M.C., K.-S.K., and H.-J.C. analyzed data; and M.-O.L., K.-S.K., and H.-J.C. wrote the paper.

The authors declare no conflict of interest.

*This Direct Submission article had a prearranged editor.

[1]Present address: Stem Cell Research Center, Korea Research Institute of Bioscience and Biotechnology, Daejeon 305-806, Korea.

[2]To whom correspondence may be addressed. E-mail: kskim@mclean.harvard.edu or hjcha@sogang.ac.kr.

This article contains supporting information online at www.pnas.org/lookup/suppl/doi:10.1073/pnas.1303669110/-/DCSupplemental.

us with a molecular strategy to selectively eliminate undifferentiated hPSCs. Indeed, our gene expression analysis revealed that in undifferentiated hESCs there is biased expression of many proapoptotic genes, whereas relatively fewer antiapoptotic genes [e.g., B-cell lymphoma 10 (*BCL10*) and baculoviral IAP repeated containing 5 (*BIRC5*), encoding Bcl10 and survivin, respectively] are highly expressed, compared with their differentiated counterparts. This observation prompted us to further hypothesize that survival of undifferentiated hPSCs is highly dependent on these antiapoptotic factors and that modulating these factors may efficiently and selectively control cell death of undifferentiated hESCs. To address this, we identified potential chemical inhibitors of these antiapoptotic factors and assessed their effects in vitro and in vivo. Remarkably, we found that a short exposure of a mixed population of hPSC-derived cells to inhibitors of survivin, such as quercetin (QC) or YM155, is sufficient to eliminate remaining undifferentiated hPSCs without affecting their differentiated counterparts, leading to complete inhibition of teratoma formation after transplantation. Moreover, differentiated cell types from hPSCs [i.e., dopaminergic neuronal cells and smooth-muscle cells (SMCs)] survived well and retained their function after exposure to QC or YM155. Furthermore, we found that, upon exposure to QC, p53 prominently accumulated in mitochondria, triggering the intrinsic apoptotic pathway in undifferentiated hPSCs. Our data illustrate the "proof of concept" that small-molecule targeting of hPSC-specific antiapoptotic factors is an efficient strategy to eliminate the risk of teratoma formation in pluripotent stem cell-based therapy.

Results

Gene Expression Profiles of Pro- and Antiapoptotic Factors in Undifferentiated vs. Differentiated hESCs. To better understand the unique cellular/molecular properties of apoptotic responses in hPSCs, we examined and compared the apoptotic machinery in undifferentiated and differentiated hESCs. Toward this goal, we prepared mRNAs from undifferentiated and spontaneously differentiated hESCs [day-14 embryoid bodies (EBs)] and examined gene expression profiles of 58 pro- and 26 antiapoptosis genes using a commercially available apoptosis PCR array (SABiosciences; *Materials and Methods*). As shown in Table S1, 22 of 58 proapoptotic genes were significantly up-regulated (>twofold) in undifferentiated hESCs compared with differentiated cells. Remarkably, among these genes, 11 (19%) were up-regulated more than 20-fold in undifferentiated hESCs (Fig. 1*A*, circled in red). Among 26 antiapoptotic genes tested here, 10 antiapoptotic genes were up-regulated more than twofold, and only two genes (8%) were up-regulated more than 10-fold. Five genes up-regulated >fivefold are highlighted by blue circles in Fig. 1*B*. These results indicate that proapoptotic genes are more preferentially expressed in undifferentiated hESCs than antiapoptotic genes, which corroborates with their hypersensitive apoptotic response to genotoxic challenges. To further examine hESC-specific expression of antiapoptotic genes, we analyzed the expression pattern of these up-regulated antiapoptotic genes and *BIRC5,* which has been reported to be expressed in ESCs (23, 26, 27), using a database library of gene expression profile (http://nextbio.com). Microarray data showing the expression levels of up-regulated (>twofold) antiapoptotic genes (*BCL10*, *BCL2L2*, *BRAF*, *BAG1*, *DFFA*, *BAG4*, *MCL1*, *BFAR*, *BCL2*, *BIRC6*, and *BIRC5*) were compared between 27 hESC lines, 26 adult stem/progenitor cells, and 16 normal noncancer cell lines (Fig. 1*C* and Table S2). Remarkably, we found that expression of only two genes, *BCL10* and *BIRC5* (encoding Bcl10 and survivin, respectively), is significantly higher in hESCs cell lines than in other cell types (e.g., tissue-specific stem cells and nontransformed cell lines). In agreement with these results, the *BIRC5* (survivin) gene was initially identified as an antiapoptotic gene that is highly expressed during fetal development but undetectable in terminally differentiated tissues (28). Furthermore, recent studies showed that it is also highly expressed in mouse and human ESCs (23, 26, 27). To further validate the specific expression of these genes during in vitro differentiation of hESCs, we monitored their mRNA expression level at different stages of in vitro differentiation [ESC, EB, neural progenitor (NP), and differentiated neuronal stages (ND)] (29). As shown in Fig. 1*D*, *BIRC5* and *BCL10* expression gradually and rapidly decreased in a pattern similar to that of *NANOG* and *OCT4*. Taken together, we propose that survivin and Bcl10 are antiapoptotic factors that are preferentially expressed in hESCs.

Blocking Survivin or Bcl10 by Specific Chemical Inhibitors Induces Selective Apoptosis of Undifferentiated hPSCs. The above findings prompted us to hypothesize that survival of undifferentiated hPSCs depends on survivin and Bcl10, and thus blocking survivin and/or Bcl10 function(s) may efficiently and selectively induce apoptosis of undifferentiated hPSCs. To test this hypothesis, we treated undifferentiated hESCs and terminally differentiated human dermal fibroblast (hDF) with chemical inhibitors such as ABT737 (BH3 domain mimetic chemical inhibitor of Bcl-2 family proteins) (30) and QC (antagonist of survivin) (31). We also tested GDC0879, a B-Raf inhibitor (32), because it is one of numerous antiapoptotic factors that were up-regulated in our initial screening but were inconsistent in multiple cell line data analysis (Fig. 1*C*). As shown in Fig. 2*A*, treatment with ABT737 or QC, but not with GDC0879, induced robust apoptotic cell death selectively in undifferentiated hESCs, supporting the importance of Bcl10 and survivin but not B-Raf for their survival. Consistent with this result, induction of the active form of caspase-3 was distinctively observed in undifferentiated hESCs after treatment with ABT737 and QC, but not with GDC0879 (Fig. 2*B*). Nanog levels were significantly down-regulated after ABT737 or QC treatment (Fig. S1*F*). In contrast, such apoptotic response was not observed in hDFs, demonstrating that ABT737 and QC induced apoptotic cell death in a pluripotent cell-specific manner. When hESCs were treated with QC, *BIRC5* mRNA expression was diminished by more than 40% and 60% when examined at 8 h and 24 h, respectively (Fig. S1*A*). When hESCs were treated with YM155, survivin mRNA expression was more robustly diminished to less than 40% level at 8 h after treatment (Fig. S1*B*), suggesting that YM155 may be a more potent survivin inhibitor than QC. To address whether selective cell death of hESCs by QC or YM155 treatment is through decreased survivin expression or other off-target effect, we next tested the effect of survivin/BIRC5 knockdown in hESCs. As shown in Fig. S1*C*, survivin/BIRC5 knockdown by siRNA significantly increased cell death of hESCs. Taken together, these results strongly suggest that QC/YM155 treatment induces selective cell death of hESCs, at least in part, via suppression of survivin gene expression.

We next tested whether ABT737 and QC have similar effects on undifferentiated hESCs and hiPSCs. First, we treated undifferentiated hESCs and their differentiated counterparts (hDFs) with different concentrations of ABT737 and QC. As shown in Fig. 2*C* (*Left*) ABT737 induced ~50% cell death of undifferentiated hESCs at 5 μM and >85% at 20 μM, but did not affect hDFs at concentrations up to 20 μM. Similarly, ABT737 induced robust cell death of undifferentiated hiPSCs but not of their differentiated counterparts, human aortic vascular SMCs (hASMCs), which originate the hiPSCs (33) (Fig. 2C, *Right*). Notably, however, ABT737 was significantly cytotoxic to hASMCs at the >5-μM range, although much less than for undifferentiated hiPSCs. In contrast, we found that QC induced specific cell death of hESCs and hiPSCs, with negligible cytotoxicity to differentiated cells (i.e., hDFs and hASMCs) at concentrations up to 50 μM (Fig. S1*G*). The differential cytotoxicity to SMCs between QC (at 50 μM, IC_{50} of hiPSCs cell death) and ABT737 (at 5 μM, IC_{50} of hiPSCs cell death) was further demonstrated by FACS analysis (Fig. 2*D*). Because ABT737 is known to inhibit broader BCL2 family proteins (30), this relatively low selectivity may underlie the observed ABT737's variable cytotoxicity to differentiated cell types. Identification of highly selective inhibitor(s) of Bcl10 will be useful

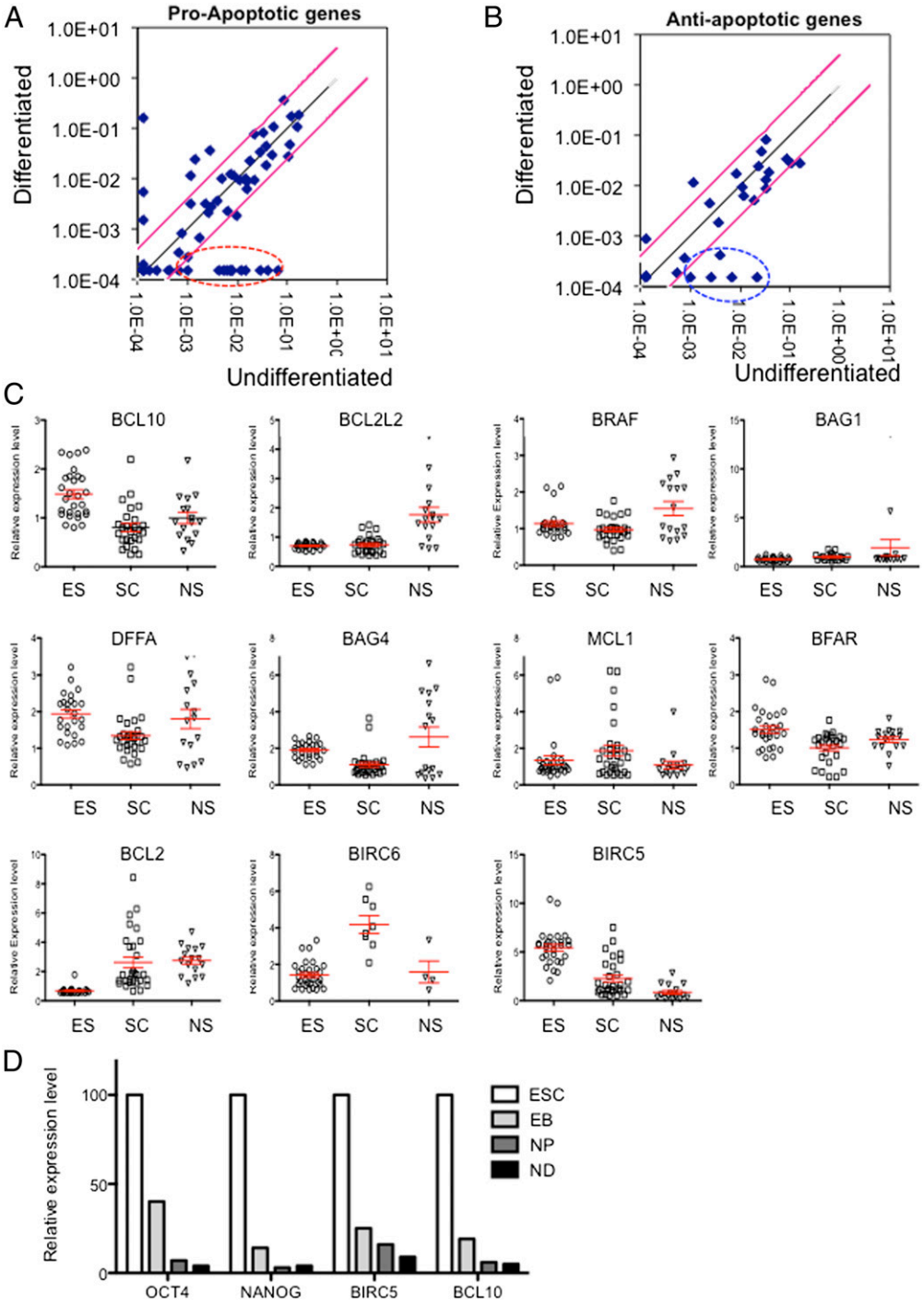

Fig.1. Analysis of pro- and antiapoptotic gene expression in undifferentiated hESCs. Expression profile analysis of proapoptotic genes (*A*) and antiapoptotic genes (*B*) through apoptosis superarray comparison between hESCs and differentiated cells (day-14 EB) from hESCs was performed, and significantly altered gene expression is shown. Dots circled with a red dotted line indicate proapoptotic genes with a more than 20-fold change (*A*). A blue dot with a circle indicates antiapoptotic genes with a more than fivefold change (*B*). (*C*) Expression level of 10 antiapoptotic factors highly expressed in undifferentiated hESCs was compared with normal cell lines and tissue-specific stem cells (adult stem cells) revealed by database search (www.nextbio.com), and relative expression level was presented in the mean value of scatter plot. Each cell line listed in the database search is described in Table S2. (*D*) *BIRC5* and *BCL10* expression of indicative cell types derived from hESCs [ESC, EB, NP, and differentiated neuronal stages (ND)] were determined by real-time RT-PCR analysis. *NANOG* and *OCT4* were used as pluripotency markers.

for more selective apoptosis of undifferentiated hPSCs. Because QC induced selective cell death of undifferentiated hESCs with no apparent cytotoxicity to both differentiated cell types up to 50 μM, we focused on the effects of QC in subsequent experiments.

QC Induces Mitochondrial Accumulation of p53 and Mitochondria-Mediated Selective Cell Death in Undifferentiated hESCs. We next tested the effect of QC on undifferentiated hESCs and differentiated hDFs. As shown in Fig. 3*A*, QC treatment induced marked cell death of undifferentiated hESCs in a dose-dependent

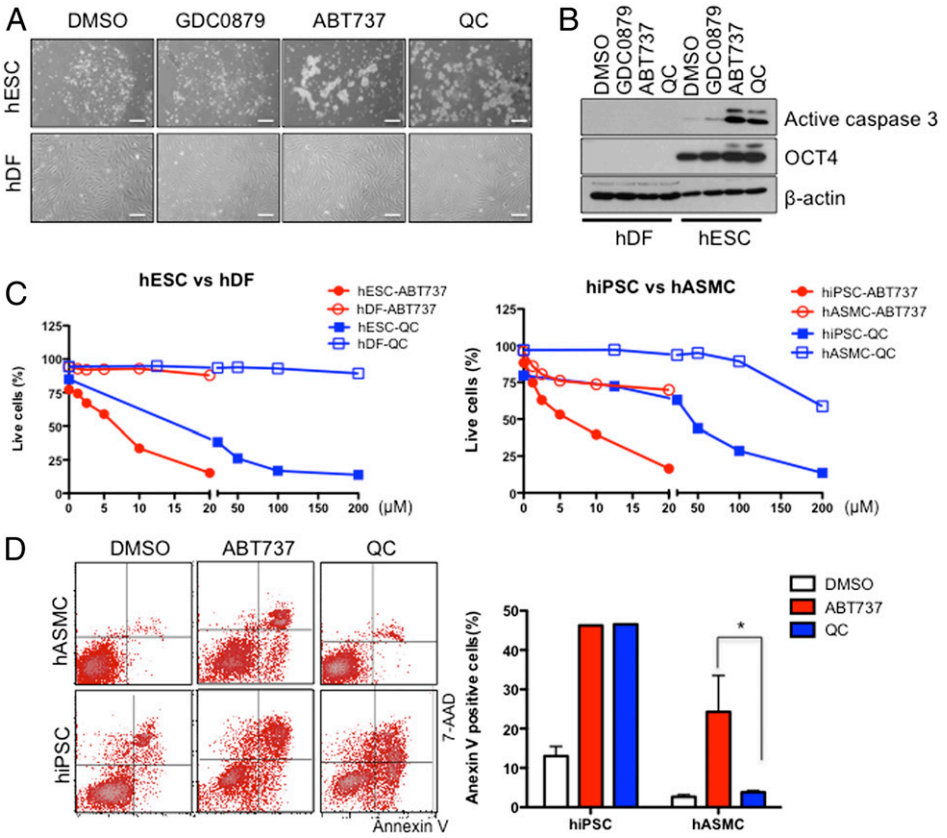

Fig. 2. Identification of small molecules inducing selective cell death of hESCs. (*A*) GDC0879 (10 μM, B-Raf inhibitor), ABT737 (10 μM, pan-BCL2 family inhibitor), or QC (100 μM, survivin inhibitor) were added to hESC and hDF cultures for 24 h. Morphological changes in hESCs and hDFs are presented by light microscopic images. (Scale bars, 200 μm.) (*B*) The level of active caspase-3 in response to the indicated small-molecule inhibitor treatment was determined by immunoblotting. Oct4 and β-tubulin were used to identify hESCs and ensure equal protein loading, respectively. (*C*) Percentages of live cells [propidium iodide (PI) negative and annexin V negative] in hESC vs. hDF and hiPSC vs. hASMC after the indicated treatments with ABT737 and QC. (*D*) Flow cytometry plots of annexin V and 7-amino-actinomycin D (7-AAD) staining after treatment with 5 μM ABT737 and 50 μM QC. Annexin V-positive cells were represented by bar graph. $*P < 0.05$. Experiments were performed at least three times, resulting in the same pattern.

manner, but not that of their differentiated counterparts, hDFs. In addition, selective cleavage of poly (ADP ribose) polymerase-1 (PARP-1) and activation of caspase-9 occurred only in undifferentiated hESCs, implying the involvement of a distinct mitochondria-mediated apoptotic event (Fig. 3*B*). Indeed, we found that caspase-3 activity, which occurs through caspase-9 activation, was increased in QC-treated hESCs in a dose-dependent manner (Fig. 3*C*).

To further understand the molecular mechanism of QC-induced selective cell death in hESCs, we investigated p53 accumulation in mitochondria, which is strongly associated with apoptotic events in mouse and human ESCs (19, 22). Considering hESCs' high susceptibility to apoptotic stimuli and dominant mitochondrial apoptotic events, we speculated that QC may induce specific cell death in hESCs through the mitochondrial apoptotic pathway. To test this possibility, we investigated whether QC induced mitochondrial accumulation of p53 in hESCs, which is known to be critical to trigger mitochondria-dependent apoptosis (19, 22, 34). We first validated the hESCs' mitochondrial fraction by establishing the specific expression of mitochondrial marker proteins [e.g., voltage-dependent anion channel (VDAC)] but not that of cytoplasmic proteins (e.g., ERK2) and nuclear protein (e.g., PARP-1) (Fig. 3*D*) under normal (untreated) conditions. After treatment with QC, we observed rapid mitochondrial accumulation of p53, as well as rapid release of the second mitochondria-derived activator of caspase/direct inhibitor of apoptosis-binding protein with low pI (Smac/DIABLO) into the cytoplasm (Fig. 3*E*), which amplifies the apoptotic signal (35). These cellular changes by QC occurred only in hESCs but not in hDFs (Fig. 3*E*). Furthermore, mitochondrial accumulation of p53 and consequent Smac/DIABLO release into the cytoplasm after QC treatment triggered caspase-9 activation in hESCs but not in hDFs (Fig. 3 *B* and *F*). Our results are consistent with previous reports showing that survivin is associated with Smac/DIABLO in mitochondria and delays its release into the cytoplasm (36, 37) and further support the notion that QC induces mitochondria-mediated apoptosis of undifferentiated hESCs via survivin. Because PTM of p53 was suggested to be important for localization of p53 under stress condition (19, 38, 39), we next compared PTM of p53 (phosphorylation and acetylation with commercially available antibodies) between hESCs and spontaneously differentiated counterparts. Of note, the PTM of p53 in hESCs after QC was significantly different from that of the differentiated counterpart (Fig. S2*A*, *Left*), which may account for mitochondrial accumulation of p53 in hESCs (19).

QC Induces Selective Cell Death of Residual Pluripotent Cells Without Affecting Differentiated Cells and Prevents Teratoma Formation After Transplantation of hPSC-Derived Cells. To test whether QC can efficiently eliminate residual undifferentiated hPSCs, we spontaneously differentiated hESCs for 6 d on a Matrigel plate to obtain a mixed cell population. This partially differentiated population contains both undifferentiated and differentiated cells, as evidenced by Oct4 positive (dotted line) and Oct4 negative (solid line) populations, respectively (Fig. 4*A*). Then we treated this mixed cell population with QC for 24 h. In contrast to undifferentiated hESCs, which underwent QC-induced cell death

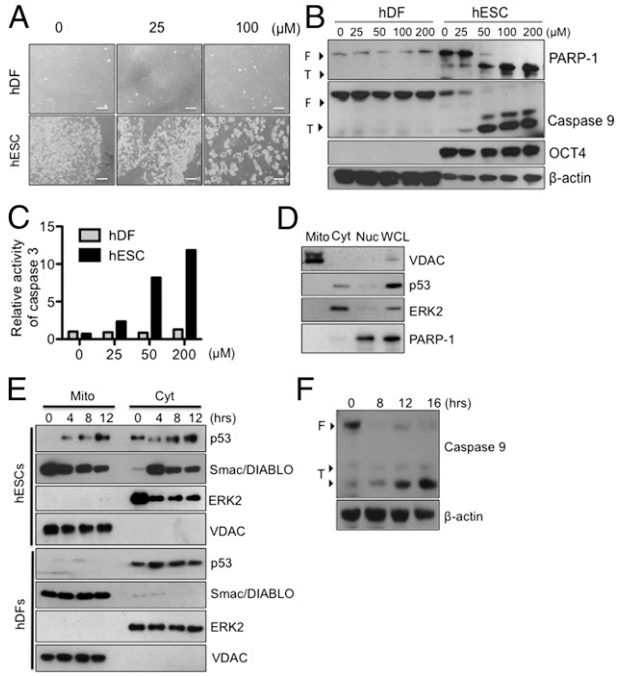

Fig. 3. Mitochondrial accumulation of p53 and apoptosis induced by QC. (*A*) Light microscopic images of hESCs and hDFs at 16 h after QC treatment. (Scale bars, 200 μm.) (*B*) Apoptotic levels were determined by immunoblotting for PARP-1 and caspase-9 cleavage (F, full length; T, truncated). Oct4 was used as an indicator of pluripotent hESCs, and β-actin was used to show equal protein loading. (*C*) Caspase-3 activity of hESCs and hDFs in response to the indicated QC treatments was determined using a caspase-3 activity assay. (*D*) Undifferentiated hESCs were fractionated into cytoplasmic (Cyt), nuclear (Nuc), and mitochondrial (Mito) fractions, and levels of appropriate marker proteins were determined in the fractions and compared with those from whole cell lysate (WCL) by immunoblotting. (*E*) Undifferentiated hESCs and hDFs were treated with 50 μM QC for the indicated times, and mitochondria were isolated at the end of treatment. Levels of p53 and Smac in mitochondria (Mito) and cytoplasm (Cyt) were determined by immunoblotting. ERK2 and VDAC were used to verify equal loading of cytoplasmic and mitochondrial fractions, respectively. (*F*) The mitochondria-dependent apoptotic signal was determined by measuring the cleaved form of caspase-9 at the indicated times after QC treatment initiation (50 μM) of undifferentiated hESCs. β-actin was used to illustrate equal loading.

(Fig. 2), the mixed population contained both QC-sensitive and QC-resistant cells. Notably, active caspase-3–positive apoptotic cells were primarily Oct4 positive (Fig. 4*A*, solid line), whereas caspase-3–negative cells were Oct4 negative (Fig. 4*A*, dotted line), confirming the highly selective cell death of pluripotent cells induced by QC among the mixed population. In addition, alkaline phosphatase (AP)-positive cells, representing PSCs, were selectively detached and underwent cell death, whereas AP-negative cells remained attached and survived (Fig. S2*B*). When hESCs were maintained without bFGF2 for 6 d we consistently observed that a number of cells survived after QC treatment as opposed to when they were maintained with bFGF2 (Fig. S2*C*).

Furthermore, apoptotic cells with distinct PARP-1 cleavage and Oct4 expression were prominently detected only in floating dead/dying cells, whereas they were absent in adherent live cells (Fig. S2*D*). Together, our results demonstrate that QC treatment induced selective cell death in remaining pluripotent cells (Oct4/AP positive), whereas differentiated cells (Oct4/AP negative) were not affected.

To further validate selective cell death of undifferentiated hESCs by QC, we mixed spontaneously differentiated hESCs (EB day 10) and undifferentiated hESCs, followed by QC treatment for 24 h. Stage-specific embryonic antigen-3 (SSEA-3)–positive cells, representing undifferentiated human ESCs, but not SSEA-3–negative cells, underwent severe cell death after QC treatment (Fig. 4*B*). We also tested the long-term effect of QC on differentiated cells (EB day 10) by analyzing cell death after a single 24-h treatment followed by 5 d in culture. As shown in Fig. S2*E*, FACS analysis revealed that the SSEA-3–positive population was almost completely eliminated, whereas the SSEA-3–negative population survived.

We next tested whether QC treatment affects the functionality of differentiated cells. First, we tested whether QC treatment skews differentiation of hESCs into specific lineages. To this end, spontaneously differentiated hESCs (EB day 10) were exposed to QC for 24 h and further differentiated for 5 additional days before PCR analyses using lineage-specific primers. As shown in Fig. 4 *C* and *D*, mRNA expression levels of the α-fetoprotein (*AFP*, an endodermal marker), the *BrachyuryT* (a mesodermal marker), and *PAX6* (an ectodermal marker) were unaffected by QC treatment, indicating that specific lineage differentiation is not affected by QC treatment. Examination of additional lineage-specific marker genes confirmed that QC or YM155 treatments have minimum effect on the differentiation process (Fig. S3 *A* and *B*). We also differentiated hESCs into a Tuj1-positive neuronal population containing a high proportion of dopamine neurons, according to our efficient in vitro differentiation method (29). After QC treatment (50 μM) for 24 h, these neuronal cells remained morphologically intact and revealed a comparable number of tyrosine hydroxylase (TH)-positive dopamine neurons (Fig. S2*F*). In addition, as examined by dopamine uptake function, these neurons remained fully functional after QC treatment (Fig. S2*G*). We also differentiated hiPSCs derived from hASMC into SMCs (hiPSC-SMC1 and -SMC3) (33) and tested the effect of QC treatment. Similarly to hESCs, apoptotic cell death occurred only in undifferentiated hiPSCs, whereas differentiated cells (hiPSC-SMCs) were unaffected (Fig. S4*A*). PARP-1 cleavage correlated with the generation of active caspase-9 and caspase-3 in hiPSCs after QC treatment but not in hiPSC-SMCs (Fig. S4*B*). Similarly, the active caspase-3–positive population after QC treatment in hiPSCs-SMCs mixed cell population was dominant in an SSEA4–positive population but not an α-smooth muscle actin (α-SMA), an SMC-specific marker, positive population (Fig. S5). Furthermore, after QC exposure, SMCs derived from hiPSCs were fully functional, as evidenced by α-SMA (Fig. S4*C*) and the induction of calcium influx (Fig. S4*D*). Taken together, our results demonstrate that QC treatment affected neither survival nor functional characteristics of hPSC-derived differentiated cells such as dopamine neurons or SMCs.

The above promising results prompted us to test whether QC treatment can prevent teratoma formation in vivo after transplantation of hPSC-derived cells. First, we treated a mixed cell population (1:1 of EB day 10 and undifferentiated hESCs) with 50 μM of QC for 24 h and injected 5×10^6 cells into mouse testes. After 10 wk, mouse testes injected with mixed cells untreated with QC developed teratomas more than 2 cm in diameter (Fig. 4*E*). In sharp contrast, mouse testes injected with QC-pretreated cells did not form any teratoma-like tumor mass. Human cells surviving in the mouse testes were identified by both immunohistochemistry (IHC) and FISH analysis. Human nuclear antigen–positive cells were found in the testes when both hESC-derived cells with and without QC treatment were transplanted (Fig. 4*F*). As expected, much more human nuclear antigen–positive cells were found in the testes grafted with QC-unexposed cells than those with QC-exposed cells. To avoid IHC bias, cells derived from hESCs (H9: 46,XX) were analyzed by FISH analysis using human X (CEP X, green) and Y (CEP Y, orange) chromosome probes. hESC-derived cells positive for the X chromosome, but not the Y chromosome, were found more prevalently in the testes with teratoma (Fig. 4*G*). Together, both QC-exposed and QC-unexposed hESC-derived cells survived after transplantation into mouse testes, but uncontrolled teratoma formation was completely inhibited when QC-exposed cells were grafted. Finally, to further evaluate the potency of QC treatment, we injected 5×10^6 undifferentiated hESCs with or

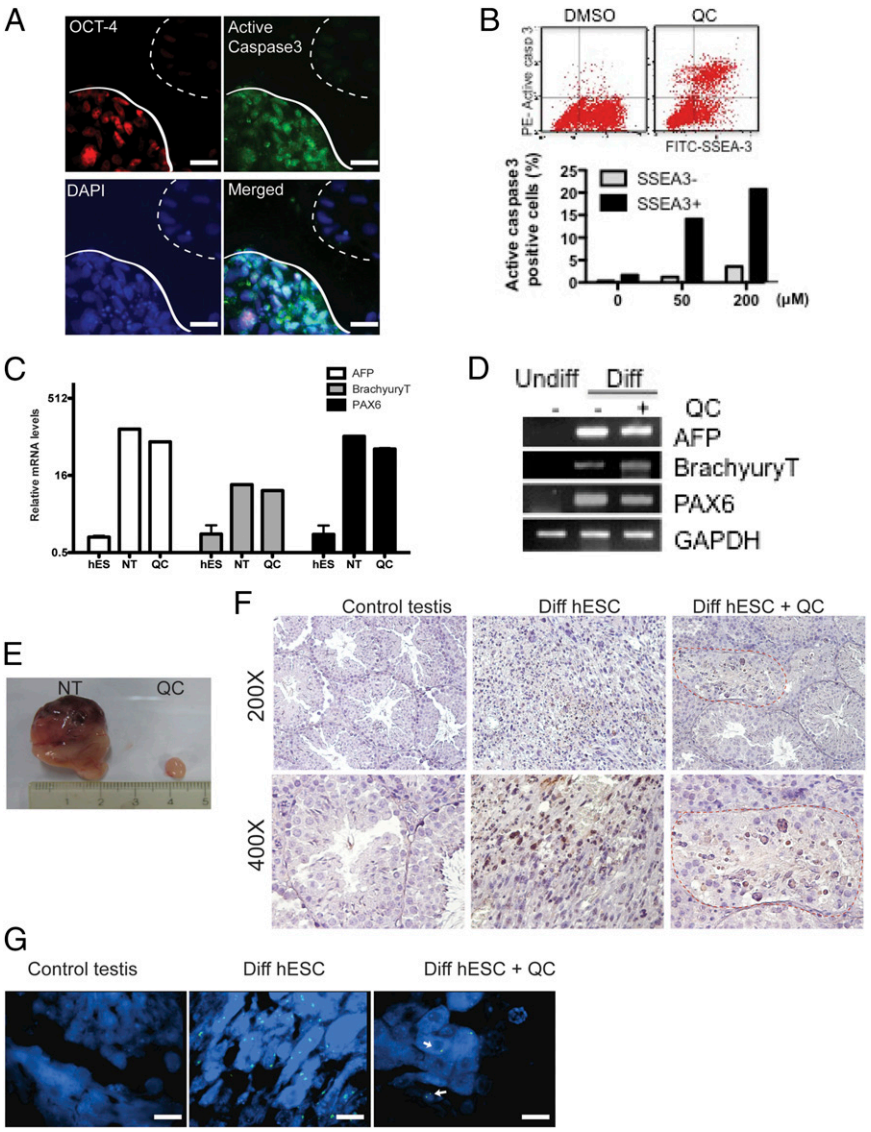

Fig. 4. QC treatment blocks teratoma formation from undifferentiated hESCs without affecting lineage-specific differentiation. (*A*) OCT-4 (red), active caspase-3 (green), and DAPI (blue) IFC images of differentiated hESCs (spontaneous differentiation for 5 d) after treatment with 50 μM QC for 24 h. (Scale bars, 50 μm.) (*B*) FACS analysis of active caspase-3 and SSEA-3 (*Left*). Quantification of the active caspase-3–positive population between SSEA-3-positive and -negative populations is graphically presented (*Right*). (*C* and *D*) The relative expression levels of lineage-specific differentiation markers (*AFP* for endoderm, *Brachyury T* for mesoderm, and *PAX6* for ectoderm) of spontaneously differentiated hESCs in the presence (QC) or absence (NT) of 100 μM QC for 24 h, compared with undifferentiated hESCs, were analyzed by (*C*) real-time PCR and (*D*) RT-PCR. (*E*) hESCs were injected into mouse testes, as shown in *B*. Representative images of teratomas formed in mouse testes injected with hESCs without (NT) or with 50 μM QC-pretreatment (QC). (*F*) Mouse testis tissues were immune-stained with anti-human nuclear antigen and observed at the indicated magnification. The red circle indicates the area where human nuclear antigen-positive cells (dark brown) were detected. (*G*) Representative FISH images stained with CEP X (α satellite, Spectrum Green) and CEP Y (Satellite III, Spectrum Orange) DNA probes. White arrows indicate human X chromosome-positive signals. (Scale bars, 25 μm.) The same results were obtained in three independent experiments.

without QC treatment (50 μM) for 24 h. Big teratomas were generated in all three mice after injection of undifferentiated hESCs into testes (Fig. S6*A*, *Top*). These teratomas contained tissues of all three germ layers (Fig. S6*B*). Similar results were obtained when hESCs were s.c. injected (Fig. S6*A*, *Middle*) and with hiPSCs using testes injection (Fig. S6*A*, *Bottom*). Thus, teratomas were generated when undifferentiated hESCs were injected into testes ($n = 4$) and the dorsum ($n = 1$) and when undifferentiated hiPSCs ($n = 1$) were injected into testes. In sharp contrast, pretreatment with QC completely prevented teratoma formation in all six corresponding injections of hPSCs (Fig. S6*C*).

Another Survivin Inhibitor, YM155, Efficiently Induces Selective Cell Death of hPSCs at the Nanomolar Range. To further validate the effectiveness of survivin inhibition for selective cell death of hPSCs, we sought to identify additional candidate inhibitor(s) of survivin. During the last decade, survivin has been extensively investigated as a potential cancer target, and a fair number of inhibitors have been identified and comprehensively tested for their potential anticancer activities (40). Among these known survivin inhibitors, we examined candidate chemicals such as gambogic acid (GA) (41), kaempferol (KP) (42), and YM155 (43) for their effectiveness to selectively induce cell death of hPSCs, in comparison with the effect of QC. Interestingly, we found that YM155, but not GA or KP, efficiently induced cell death of hESCs (Fig. 5*A*). We next tested the dose dependent response of YM155 for inducing cell death of hESCs (Fig. 5 *B* and *C*). Remarkably, YM155's IC_{50} was found to be less than 5 nM (approximately 2.5 nM, IC_{50} of YM155) for inducing hESCs' cell death (Fig. 5*D*). Thus, YM155 was effective at a concentration three orders of magnitude lower than QC. Moreover, YM155 seemed to be noncytotoxic to differentiated cells such as hDFs and hASMCs (Fig. 5*D*). At a concentration up to 250 nM (100 times higher concentration than the IC_{50} for hiPSCs), SMCs survived well without any sign of cell death (Fig. 5*D*). We next treated a mixed cell population (1:1 of spontaneously differentiated EB day 10 and undifferentiated hESCs) with 10 nM of YM155 for 24 h and analyzed their apoptotic responses after 6 d of additional differentiation by FACS analysis (Fig. 5*E*). In the absence of YM155 treatment, ~30% of SSEA-3^+ cells were retained at day 6 (Fig. 5*E*). In sharp contrast, exposure to YM155 reduced the SSEA-3^+ cells to undetectable levels. When hDFs were treated with YM155, there was apparently no cell death (Fig. S7*A*). Cell death of hESCs by YM155 was selectively occurring in SSEA-3^+ cells (Fig. S7*B*). YM155 treatment induced different PTM of p53 from that of a differentiated counterpart, similar to the case with QC treatment (Fig. S2*A*, *Right*). Finally,

as expected, in hESCs pretreatment with YM155 for 24 h was sufficient to inhibit teratoma formation (Fig. 5*F*). Furthermore, Tuj1+/TH+ dopamine neurons derived from hESCs remained intact neuronal morphology after 24 h treatment of YM155 (Fig. S7*C*), which appear to be functionally intact, as examined by dopamine uptake function (Fig. S7*D*). In addition, as determined by Ca^{2+} influx, SMC derived from hiPSCs was functionally intact after treatment with YM155 (Fig. 5*H*). Similar to the case with QC, teratoma derived from cell mixture of hiPSCs and SMCs (Fig. S7 *E* and *F*) was completely inhibited by single

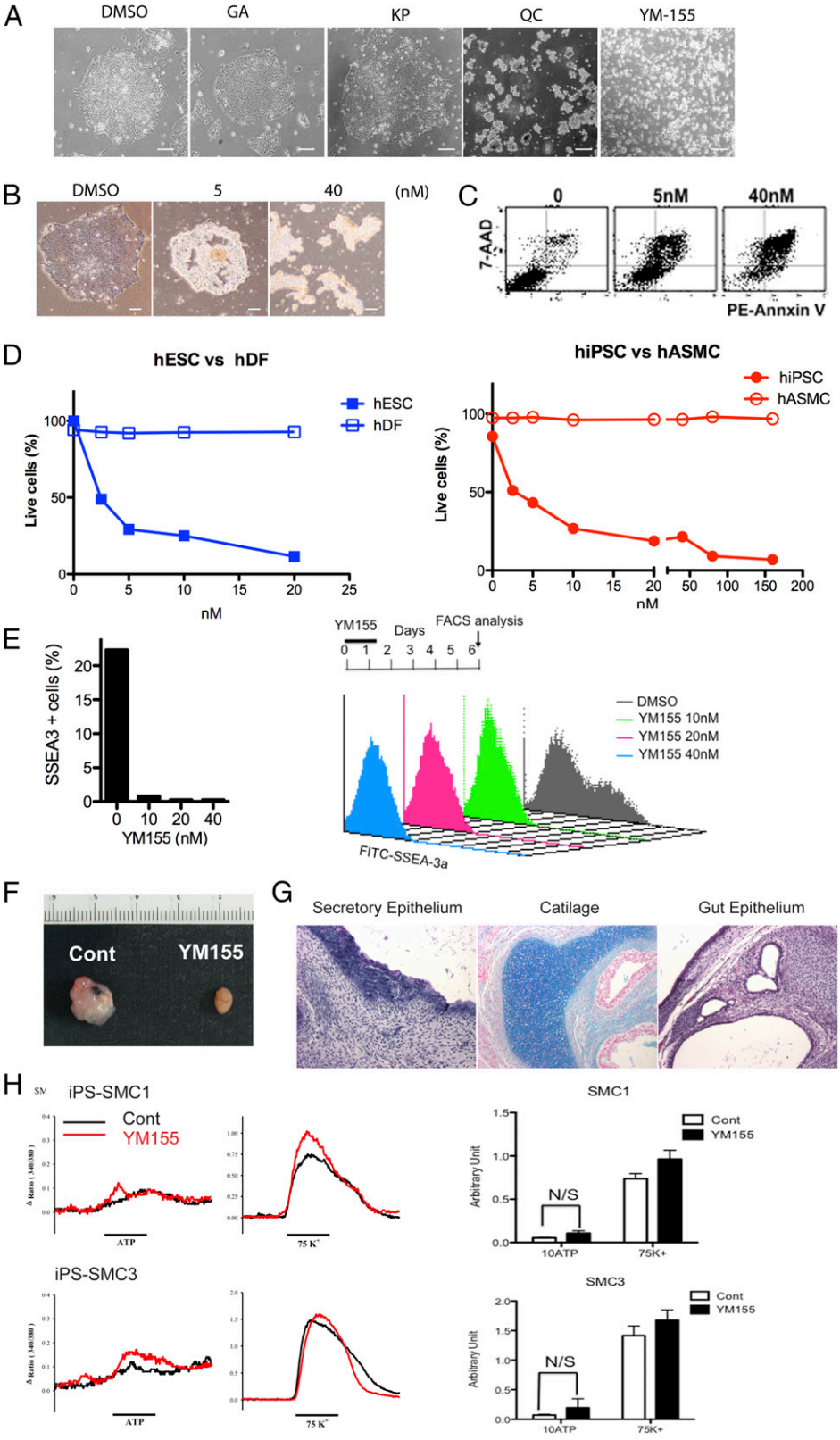

Fig. 5. Effect of another survivin inhibitor, YM155, on selective cell death of hiPSCs and teratoma formation. (*A*) Light microscopic images of hESCs after treatment with the indicated survivin inhibitors for 24 h: 200 μM of GA, 200 μM of KP, 50 μM of QC, and 10 nM of YM155. (Scale bars, 200 μm.) (*B*) Representative light microscopic images of hESCs at each dosage level. (Scale bars, 200 μm.) (*C*) Flow cytometry plots of annexin V and 7-AAD staining after treatment with indicated dose of YM155. (*D*) Graphical presentation of the percentage of live cells assayed by measuring cells negative for annexin V and 7-AAD. (*E*) FACS analysis of mixed cell population stained with FITC-SSEA-3 (*x* axis) after 5 d with a single treatment with the indicated dose of YM155 (24 h), followed by 5 additional days differentiation. A graph representing the resulting SSEA-3–positive cell is presented (*Right*). (*F*) Teratoma formation of hESCs injected into mouse testes with or without pretreatment with 10 nM of YM155. (*G*) Sections of teratomas generated by hESCs are shown stained with hematoxylin and eosin, Masson's trichrome, and Alcian Blue. Teratomas produced cells indicative of gut epithelium, cartilage, and secretory epithelium. (*H*) Relative change in intracellular calcium levels in response to a pharmacological agonist, ATP (20 μM; *Left*) or membrane depolarization (75 mM K^+; *Right*) in hiPSC-SMC1 (*Upper*) and hiPSC-SMC3 (*Lower*) cells. The calcium response was tested before (black line) and after (red line) treatment with 10 nM of YM155 for 24 h. Treatment with ATP or 75 mM K^+ is indicated by the black bar at the bottom of each panel. Net changes in intracellular calcium after treatment with ATP or 75 mM K^+. Changes in calcium level were expressed as the ratio (340/380) of Fura-2 emissions. Means SEM; n = 18–34. Experiments were performed at least twice, resulting in the same results.

exposure of YM155 for 24 h before injection, with no apparent sign of teratoma (Fig. S7*E*, *Right*). Taken together, two mice were subjected to examine the effect of YM155 for inhibition of teratoma formation by hPSCs (one for hESCs and one for hiPSCs) (Fig. S7*G*). None of the mice pretreated with YM155 formed teratoma, indicating that YM155 is highly effective to block teratoma formation.

Discussion

Accumulation of mutations in early embryonic cells and ESCs would result in enormous harmful effects to all subsequently derived somatic cells arising at later developmental stages and/or those of future generations. Thus, it is critical that these cells maintain their genomic integrity by establishing unique mechanisms, such as significantly lower mutation rates and lower frequencies of mitotic recombination than their differentiated counterparts (21, 44). The low mutation frequency of ESCs seems to be the result of not only being equipped with a well-developed DNA repair system (45, 46) but also of hypersensitivity to cell death under genotoxic stresses (23). Hypersensitivity to cell death under stress conditions is supposedly a protective mechanism to safeguard the genomic integrity of ESCs by removing damaged cells with a mutational burden (22). Therefore, in ESCs, stress mediators (e.g., p53) preferentially trigger apoptosis rather than induce a cell cycle arrest-related transcriptional program (22, 47). Given that p53 directly suppresses Nanog expression, one of a number of key transcription factors involved in pluripotency maintenance (48), p53-dependent transcription under genotoxic stress could induce differentiation by blocking Nanog expression, which might transmit the possible mutations under genotoxic stress condition to the differentiated cells. To avoid this outcome, p53 must be specifically regulated to preferentially induce an apoptotic response in ESCs in a p53 transcription-independent manner. In undifferentiated mouse and human ESCs p53-mediated apoptosis is a transcription-independent event, occurring through translocation of p53 into mitochondria (19, 22). Because *BIRC5* is suppressed by p53-dependent transcription in normal somatic cells (49), atypical p53 response in hPSCs (translocation to the mitochondria but not nucleus under stress condition) would result in constant high expression of *BIRC5* in undifferentiated hPSCs. To further test the possible p53 transcription-dependent apoptotic response induced by QC or YM155, we determined their effect on gene regulation of p21 and p53 inducible gene 3 (*PIG3*), a p53 downstream proapoptotic gene (50). As shown in Fig. S8*A*, QC seemed to transiently promote p21CIP1 expression, whereas YM155 did not significantly affect p21 expression. *PIG3* expression was unaffected by QC or YM155 treatment in hESCs (Fig. S8*B*), indicating that p53-dependent transcription marginally affected apoptosis induction, if at all. In addition, QC or YM155 treatment did not increase two representative NF-κB–dependent proapoptotic genes, Bcl2-interacting mediator of cell death (BIM) (51) and Fas-ligand (FASLG) (52) (Fig. S8 *C* and *D*). Taken together, to maintain such a high susceptibility to apoptotic signals, ESCs may need to be equipped with a unique molecular apoptosis machinery. Indeed, we found that undifferentiated hESCs highly express a number of proapoptotic genes and relatively few antiapoptotic genes, compared with their differentiated counterparts (Fig. 1). Among the 11 proapoptotic genes that were highly up-regulated (>20-fold) in hESCs, 6 are strongly correlated with mitochondrial apoptotic pathways: *PYCARD*, *APAF-1*, *TP53BP2*, *HRK*, *BCL2L11*, and *BNIP1* (Table S1) (53–57). Thus, in the presence of these highly expressed proapoptotic genes, hESCs are likely critically dependent, for their survival and self-renewal, on relatively few antiapoptotic genes (e.g., Bcl10 and survivin) that are highly and preferentially expressed in hESCs.

On the basis of the unique signature of pro- and antiapoptotic gene expression, we speculated that inhibiting key antiapoptotic factors would induce apoptotic cell death of residual undifferentiated hPSCs and thus prevent tumor/teratoma formation after transplantation of hPSC-derived cells. In particular, we sought to test chemical inhibitors of Bcl10 and survivin that are relatively enriched in hESCs compared with differentiated cell types (Fig. 1). Indeed, we found that ABT737 and QC, inhibiting Bcl-2 family proteins and survivin, respectively, triggered robust apoptosis of hESCs and hiPSCs but not that of their differentiated counterparts (Fig. 2). However, because ABT737 is not Bcl10-specific and exerts modest levels of nonspecific cytotoxicity to certain differentiated cell types, we focused on the effects of the survivin inhibitor QC in this study.

QC, a ubiquitous dietary flavonoid, is widely found in many fruits and vegetables, including apples and green tea. QC has been extensively investigated for its ability to inhibit the proliferation of various types of cancer cells and tumor growth, which is found to be related, at least in part, to its inhibition of survivin expression (31, 40, 58). Remarkably, QC triggered rapid and robust apoptosis only in hPSCs but not in their differentiated counterparts (Figs. 2–4). Furthermore, a single exposure of undifferentiated hESCs to QC completely prevented teratoma formation after in vivo transplantation, whereas differentiated cells derived from hPSCs survived and remained functionally intact (Fig. 4 and Figs. S2 and S4). In addition, QC treatment does not seem to influence differentiation of hESCs into three germ layer lineages (Fig. 4*C* and *D* and Fig. S3). Notably, a single exposure to QC followed by in vitro culture and differentiation was sufficient to completely prevent teratoma formation after transplantation of the resulting cells (Fig. 4*E*). In contrast, QC treatment had no effect on the survival and function of fully differentiated cells from hPSCs, such as dopamine neurons and SMCs (Figs. S2 and S4). The undifferentiated hESC-specific cell death in response to QC occurred through p53 mitochondrial accumulation, triggering mitochondrial apoptosis (Fig. 3).

Interestingly, we also found that another survivin inhibitor, YM155, which shares similar molecular structure with QC, can efficiently induce apoptotic cell death of both hESCs and hiPSCs, further validating our notion that small molecules inhibiting key antiapoptotic factors (e.g., survivin) represent a viable strategy to prevent the potential risk of tumor/teratoma formation in hPSC-based cell therapy. Surprisingly, YM155 is more potent than QC (up to three orders of magnitude) and effectively induced hPSCs cell death in the nanomolar ranges (Fig. 5), although other flavonoids, such as GA (found to be effective in mouse embryonic stem cells (Fig. S1*D*) and KP, were not effective in hESCs, considering their close structural similarity with QC (Fig. 5*A*). Transplantation of YM155-treated cells resulted in complete prevention of teratoma formation (Fig. 5*F*). In contrast, it was noncytotoxic to differentiated cells at the concentration range tested in this study (Fig. 5*D*). For instance, dopamine neurons derived from hESCs exposed to YM155 for 24 h survived well and functionally intact, as examined by dopamine uptake function (Fig. S7 *C* and *D*). Taken together, we propose that small molecules such as QC and YM155 induce selective apoptosis of residual undifferentiated hPSCs via survivin inhibition and can prevent tumor/teratoma formation in hESC- or hiPSC-based cell therapy.

With regard to safety, QC has been widely used as a nutritional supplement in the United States, and no adverse effects have been reported, even with relatively high doses (500–1,000 mg) for long periods (12 wk) (59). Furthermore, YM155 is one of a few chemicals that have been shown to be relatively safe and that moved on to phase II clinical trial (40, 60). Thus, we can expect that the karyotype of SMCs will remain normal after QC treatment (Fig. S9). However, it is also noteworthy that timely treatment with QC or YM155 for eliminating residual hPSCs before hematopoiesis (e.g., hemangioblasts development) (61) needs to be considered to minimize unexpected undesirable effects on the erythroid terminal maturation process, which requires transient survivin expression (62).

In summary, we found that hPSCs have a unique and biased signature of pro- and antiapoptotic gene expression, which may be critical for their hypersensitivity to genotoxic stimuli. In particular, two antiapoptotic genes, *BIRC5* and *BCL10*, are selec-

tively enriched in hESCs, and their inhibition leads to selective cell death of undifferentiated hPSCs but does not affect lineage-specific differentiation or functionality of differentiated cells. Furthermore, on the basis of their specific expression in ESCs and teratomas (23, 26, 27), survivin antagonists were proposed as a strategy to avoid teratoma formation for clinical application of hESCs (27). Indeed, our data show that a single exposure of hESCs or hiPSCs with such inhibitors (e.g., QC and YM155) is sufficient to eliminate tumor formation. Because hPSC-derived mixed populations can be exposed in vitro to these chemicals for a short time, washed off, and can be further differentiated, the resulting cells may represent a safe transplantable cell source with no or minimal risk for tumor/teratoma formation.

Materials and Methods

Reagents. GDC0879 (catalog no. S1104:) and ABT737 (catalog no. S1002:) were purchased from Selleck Chemicals. QC (catalog no. Q0125) was purchased from Sigma-Aldrich, and KP (catalog no. 420345) was purchased from EMD Chemicals. Gambogic acid (catalog no. sc-200137) was purchased from Santa Cruz Biotechnology.

hPSCs Cell Culture and Spontaneous Differentiation. Human ESCs (H9; Wicell Research Institute) and iPSCs (33) were maintained in ESC medium [DMEM/F12 supplemented with 20% (vol/vol) KnockOut Serum Replacement, 0.1% gentamycin, 1% nonessential amino acids, 0.1% β-mercaptoethanol, and 4 ng/mL bFGF2] on mitomycin C-treated mouse embryonic fibroblast (MEF) feeder cells. For QC treatment, hESCs or hiPSCs were cultured in mTeSR1 medium (29106; Stem Cell Technology) on Matrigel-coated 60-mm dishes, as described in the manufacturer's protocol. To construct a mixed population with undifferentiated and differentiated hESCs, we cotransferred undifferentiated hESCs and spontaneously differentiated cells by culturing with media containing 10% (vol/vol) FBS for 10 d to a Matrigel-coated dish.

Cell Culture. hDFs were cultured in high-glucose DMEM (Gibco, catalog no. 11995) with 10% (vol/vol) FBS and 0.1% gentamycin. hASMC and hiPSC-derived SMCs were cultured in SMCM medium (ScienCell Research Laboratories, catalog no. 1101), as described previously (33).

Immunoblotting and Immunofluorescence Cytochemistry. Immunoblotting analysis was performed as described previously (63). Antibodies used in the present study, anti-PARP1 (SC-7150), anti-Oct4 (SC-5279), anti-β-actin (SC-47778), and anti-ERK2 (SC-154), were purchased from Santa Cruz Biotechnology. Anti-caspase-9 (catalog no. 9502) and anti-cleaved caspase-3 (catalog no. 9661) were purchased from Cell Signaling Technology. Immunofluorescence cytochemistry (IFC) was performed as described previously (62). Primary antibodies (1:200) used for IFC were anti-Oct4 (SC-5279) and anti-cleaved caspase-3 (Cell Signaling, catalog no. 9661). Images were captured and analyzed using an Axioscope A1 microscope (Carl Zeiss).

Teratoma Formation and IHC. EBs were formed from hESCs or hiPSCs in the presence or absence of QC (100 μM) or YM155 (10 nM), for 24 h. Cells (~5×10^6 cells of hESCs or hiPSCs) were harvested and injected into the testes of nonobese diabetic/SCID mice (Charles River Laboratories). Ten weeks after injection, xenograft masses were harvested, fixed with 4% (vol/vol) paraformaldehyde for 2 wk, and embedded in paraffin using a Tissue-Tek VIP embedding machine (Miles Scientific) and a Thermo Shandon Histocenter2 (Thermo Fisher Scientific). Sections (2-μm thickness) were obtained using a Leica RN2065 microtome (Leica) and stained with hematoxylin-eosin, Masson's trichrome, and Alcian Blue, and analyzed by a trained pathologist. Mouse anti-human nuclear antigen (Thermo Scientific Pierce Antibodies, MA1-83365) was used for human nuclear antigen staining. To eliminate the possible background of mouse tissue sections, a Vector M.O.M immunodetection kit (Vector Laboratories, BMK-2200) was used according to the manufacturer's protocol. The experiments were reviewed and approved by the Institutional Animal Care and Use Committee of CHA University. All procedures were performed in accordance with the Guidelines for the Care and Use of Laboratory Animals published by the US National Institutes of Health (publication no. 85-23, revised 1996).

Differentiation of hESCs to Dopaminergic Neurons. Undifferentiated hESCs on a mitomycin C-treated MEF feeder layer were differentiated toward midbrain-type NP cells (NPCs) by culturing on an MS5 feeder layer for 10 d, and then subsequently on an MS5-SHH feeder layer for another 10 d, as previously described (29). The differentiated NPCs were maintained with DMEM/F12 (Gibco 12500) containing 3 mM D(+) glucose (Sigma-aldrich), 2 mM L-glutamine (Sigma-Aldrich), 5 mg/L insulin (Sigma-Aldrich), 50 mg/L transferrin (Sigma-Aldrich), 30 nM sodium selenite (Sigma-Aldrich), 28.5 mM sodium bicarbonate (Sigma-Aldrich), and penicillin/streptomycin (Invitrogen) and subcultured every 7 d. Terminal differentiation to dopaminergic (DA) neurons from hESC-derived NPCs was performed by culturing with ITS Supplement-A (catalog no. 07151 STEMCELL Tech) with dibutyryl cAMP (0.5 mmol/mL; Sigma-Aldrich), brain-derived neurotrophic factor (20 ng/mL), and glial cell line-derived neurotrophic factor (20 ng/mL; R&D Systems).

DA Uptake Assay. H9-derived DA neurons were treated with QC at a 50-μM concentration for 18 h, and then the ability of the DA neurons to uptake dopamine was measured as described previously (64). Briefly, the cells were incubated at 37 °C for 10 min using 50 nmol/L [3H]DA (51 Ci/mmol; Amersham) with or without 10 μmol/L nomifensine (RBI), and a dopamine transporter blocker to determine nonspecific uptake. After uptake, the reaction solution was aspirated and the cells washed with ice-cold Dulbecco's phosphate buffered saline. The cells were lysed with 0.5 mol/L NaOH, and the radioactivity from the [3H]DA uptake was measured by liquid scintillation counting (Perkin-Elmer). The amount of DA uptake was calculated by deducting nonspecific uptake (with 10 μM nomifensine) from the uptake value without nomifensine.

Calcium Measurement in Live Cells. To test calcium responses, calcium transients induced either by a pharmacological agent, ATP, or by a 75-mM K^+ solution were measured fluorometrically using the calcium indicator Fura-2 (Molecular Probes) and imaged digitally, as described previously (65).

Statistical Analysis. The graphical data were presented as mean ± SEM. Statistical significance among three groups and between groups was determined using one-way or two-way ANOVA after Bonferroni posttest and Student *t* test, respectively. Significance was assumed for $P < 0.05$ (*), $P < 0.01$ (**).

Karyotype Analysis of hMSCs. SMCs were incubated with 100 nM colcemid for 10 h and were then collected. The karyotypes were determined using a standard G-banding procedure.

Note in Proof. While under review, two articles related to this study have been published (66, 67).

ACKNOWLEDGMENTS. This work was supported by the National Research Foundation of Korea (NRF) grant funded by the Korean government (Minister of Science, Information and Communications Technology, and Future Planning) (No.2011-0030043) and Bio & Medical Technology Development Program Grant 2010-0020232 from the National Research Foundation of Korea, and by National Institutes of Health Grant NS070577.

1. Thomson JA, et al. (1998) Embryonic stem cell lines derived from human blastocysts. *Science* 282(5391):1145–1147.
2. Takahashi K, et al. (2007) Induction of pluripotent stem cells from adult human fibroblasts by defined factors. *Cell* 131(5):861–872.
3. Yu J, et al. (2007) Induced pluripotent stem cell lines derived from human somatic cells. *Science* 318(5858):1917–1920.
4. Robinton DA, Daley GQ (2012) The promise of induced pluripotent stem cells in research and therapy. *Nature* 481(7381):295–305.
5. Klimanskaya I, Rosenthal N, Lanza R (2008) Derive and conquer: Sourcing and differentiating stem cells for therapeutic applications. *Nat Rev Drug Discov* 7(2):131–142.
6. Hanna JH, Saha K, Jaenisch R (2010) Pluripotency and cellular reprogramming: Facts, hypotheses, unresolved issues. *Cell* 143(4):508–525.
7. Yu J, Thomson JA (2008) Pluripotent stem cell lines. *Genes Dev* 22(15):1987–1997.
8. Blum B, Benvenisty N (2008) The tumorigenicity of human embryonic stem cells. *Adv Cancer Res* 100:133–158.
9. Miura K, et al. (2009) Variation in the safety of induced pluripotent stem cell lines. *Nat Biotechnol* 27(8):743–745.
10. Teng X, Keys H, Yuan J, Degterev A, Cuny GD (2008) Structure-activity relationship and liver microsome stability studies of pyrrole necroptosis inhibitors. *Bioorg Med Chem Lett* 18(11):3219–3223.
11. Teng X, et al. (2007) Structure-activity relationship study of [1,2,3]thiadiazole necroptosis inhibitors. *Bioorg Med Chem Lett* 17(24):6836–6840.
12. Hu X, Han W, Li L (2007) Targeting the weak point of cancer by induction of necroptosis. *Autophagy* 3(5):490–492.

13. Feng Q, et al. (2010) Hemangioblastic derivatives from human induced pluripotent stem cells exhibit limited expansion and early senescence. *Stem Cells* 28(4):704–712.
14. Schuldiner M, Itskovitz-Eldor J, Benvenisty N (2003) Selective ablation of human embryonic stem cells expressing a "suicide" gene. *Stem Cells* 21(3):257–265.
15. Chung S, et al. (2006) Genetic selection of sox1GFP-expressing neural precursors removes residual tumorigenic pluripotent stem cells and attenuates tumor formation after transplantation. *J Neurochem* 97(5):1467–1480.
16. Tang C, et al. (2011) An antibody against SSEA-5 glycan on human pluripotent stem cells enables removal of teratoma-forming cells. *Nat Biotechnol* 29(9):829–834.
17. Choo AB, et al. (2008) Selection against undifferentiated human embryonic stem cells by a cytotoxic antibody recognizing podocalyxin-like protein-1. *Stem Cells* 26(6): 1454–1463.
18. Knoepfler PS (2009) Deconstructing stem cell tumorigenicity: A roadmap to safe regenerative medicine. *Stem Cells* 27(5):1050–1056.
19. Qin H, et al. (2007) Regulation of apoptosis and differentiation by p53 in human embryonic stem cells. *J Biol Chem* 282(8):5842–5852.
20. Wilson KD, et al. (2010) Effects of ionizing radiation on self-renewal and pluripotency of human embryonic stem cells. *Cancer Res* 70(13):5539–5548.
21. Hong Y, Cervantes RB, Tichy E, Tischfield JA, Stambrook PJ (2007) Protecting genomic integrity in somatic cells and embryonic stem cells. *Mutat Res* 614(1-2):48–55.
22. Han MK, et al. (2008) SIRT1 regulates apoptosis and Nanog expression in mouse embryonic stem cells by controlling p53 subcellular localization. *Cell Stem Cell* 2(3): 241–251.
23. Filion TM, et al. (2009) Survival responses of human embryonic stem cells to DNA damage. *J Cell Physiol* 220(3):586–592.
24. Dumitru R, et al. (2012) Human embryonic stem cells have constitutively active Bax at the Golgi and are primed to undergo rapid apoptosis. *Mol Cell* 46(5):573–583.
25. Smith AJ, et al. (2012) Apoptotic susceptibility to DNA damage of pluripotent stem cells facilitates pharmacologic purging of teratoma risk. *Stem Cells Transl Med* 1(10): 709–718.
26. Guo Y, Mantel C, Hromas RA, Broxmeyer HE (2008) Oct-4 is critical for survival/ antiapoptosis of murine embryonic stem cells subjected to stress: effects associated with Stat3/survivin. *Stem Cells* 26(1):30–34.
27. Blum B, Bar-Nur O, Golan-Lev T, Benvenisty N (2009) The anti-apoptotic gene survivin contributes to teratoma formation by human embryonic stem cells. *Nat Biotechnol* 27(3):281–287.
28. Ambrosini G, Adida C, Altieri DC (1997) A novel anti-apoptosis gene, survivin, expressed in cancer and lymphoma. *Nat Med* 3(8):917–921.
29. Rhee YH, et al. (2011) Protein-based human iPS cells efficiently generate functional dopamine neurons and can treat a rat model of Parkinson disease. *J Clin Invest* 121(6): 2326–2335.
30. Oltersdorf T, et al. (2005) An inhibitor of Bcl-2 family proteins induces regression of solid tumours. *Nature* 435(7042):677–681.
31. Kuo PC, Liu HF, Chao JI (2004) Survivin and p53 modulate quercetin-induced cell growth inhibition and apoptosis in human lung carcinoma cells. *J Biol Chem* 279(53): 55875–55885.
32. Wong H, et al. (2009) Pharmacodynamics of 2-[4-[(1E)-1-(hydroxyimino)-2,3-dihydro-1H-inden-5-yl]-3-(pyridine-4-yl)-1H-pyrazol-1-yl]ethan-1-ol (GDC-0879), a potent and selective B-Raf kinase inhibitor: Understanding relationships between systemic concentrations, phosphorylated mitogen-activated protein kinase kinase 1 inhibition, and efficacy. *J Pharmacol Exp Ther* 329(1):360–367.
33. Lee TH, et al. (2010) Functional recapitulation of smooth muscle cells via induced pluripotent stem cells from human aortic smooth muscle cells. *Circ Res* 106(1): 120–128.
34. Mihara M, et al. (2003) p53 has a direct apoptogenic role at the mitochondria. *Mol Cell* 11(3):577–590.
35. Adrain C, Creagh EM, Martin SJ (2001) Apoptosis-associated release of Smac/DIABLO from mitochondria requires active caspases and is blocked by Bcl-2. *EMBO J* 20(23): 6627–6636.
36. Ceballos-Cancino G, Espinosa M, Maldonado V, Melendez-Zajgla J (2007) Regulation of mitochondrial Smac/DIABLO-selective release by survivin. *Oncogene* 26(54): 7569–7575.
37. Song Z, Yao X, Wu M (2003) Direct interaction between survivin and Smac/DIABLO is essential for the anti-apoptotic activity of survivin during taxol-induced apoptosis. *J Biol Chem* 278(25):23130–23140.
38. Brooks CL, Gu W (2011) p53 regulation by ubiquitin. *FEBS Lett* 585(18):2803–2809.
39. Santiago A, Li D, Zhao LY, Godsey A, Liao D (2013) p53 SUMOylation promotes its nuclear export by facilitating its release from the nuclear export receptor CRM1. *Mol Biol Cell*, 10.1091/mbc.E12-10-0771.
40. Altieri DC (2008) Survivin, cancer networks and pathway-directed drug discovery. *Nat Rev Cancer* 8(1):61–70.
41. Wang T, et al. (2008) Gambogic acid, a potent inhibitor of survivin, reverses docetaxel resistance in gastric cancer cells. *Cancer Lett* 262(2):214–222.
42. Siegelin MD, Reuss DE, Habel A, Herold-Mende C, von Deimling A (2008) The flavonoid kaempferol sensitizes human glioma cells to TRAIL-mediated apoptosis by proteasomal degradation of survivin. *Mol Cancer Ther* 7(11):3566–3574.
43. Nakahara T, et al. (2007) YM155, a novel small-molecule survivin suppressant, induces regression of established human hormone-refractory prostate tumor xenografts. *Cancer Res* 67(17):8014–8021.
44. Stambrook PJ (2007) An ageing question: Do embryonic stem cells protect their genomes? *Mech Ageing Dev* 128(1):31–35.
45. Maynard S, et al. (2008) Human embryonic stem cells have enhanced repair of multiple forms of DNA damage. *Stem Cells* 26(9):2266–2274.
46. Luo LZ, et al. (2012) DNA repair in human pluripotent stem cells is distinct from that in non-pluripotent human cells. *PLoS ONE* 7(3):e30541.
47. Zhao T, Xu Y (2010) p53 and stem cells: New developments and new concerns. *Trends Cell Biol* 20(3):170–175.
48. Lin T, et al. (2005) p53 induces differentiation of mouse embryonic stem cells by suppressing Nanog expression. *Nat Cell Biol* 7(2):165–171.
49. Mirza A, et al. (2002) Human survivin is negatively regulated by wild-type p53 and participates in p53-dependent apoptotic pathway. *Oncogene* 21(17):2613–2622.
50. Venot C, et al. (1998) The requirement for the p53 proline-rich functional domain for mediation of apoptosis is correlated with specific PIG3 gene transactivation and with transcriptional repression. *EMBO J* 17(16):4668–4679.
51. Wang Z, Zhang B, Yang L, Ding J, Ding HF (2008) Constitutive production of NF-kappaB2 p52 is not tumorigenic but predisposes mice to inflammatory autoimmune disease by repressing Bim expression. *J Biol Chem* 283(16):10698–10706.
52. Matsui K, Fine A, Zhu B, Marshak-Rothstein A, Ju ST (1998) Identification of two NF-kappa B sites in mouse CD95 ligand (Fas ligand) promoter: Functional analysis in T cell hybridoma. *J Immunol* 161(7):3469–3473.
53. Ohtsuka T, et al. (2004) ASC is a Bax adaptor and regulates the p53-Bax mitochondrial apoptosis pathway. *Nat Cell Biol* 6(2):121–128.
54. Kobayashi S, et al. (2005) 53BP2 induces apoptosis through the mitochondrial death pathway. *Genes Cells* 10(3):253–260.
55. Perkins CL, Fang G, Kim CN, Bhalla KN (2000) The role of Apaf-1, caspase-9, and bid proteins in etoposide- or paclitaxel-induced mitochondrial events during apoptosis. *Cancer Res* 60(6):1645–1653.
56. Sunayama J, et al. (2004) Physical and functional interaction between BH3-only protein Hrk and mitochondrial pore-forming protein p32. *Cell Death Differ* 11(7): 771–781.
57. Gressner O, et al. (2005) TAp63alpha induces apoptosis by activating signaling via death receptors and mitochondria. *EMBO J* 24(13):2458–2471.
58. Priyadarsini RV, et al. (2010) The flavonoid quercetin induces cell cycle arrest and mitochondria-mediated apoptosis in human cervical cancer (HeLa) cells through p53 induction and NF-kappaB inhibition. *Eur J Pharmacol* 649(1-3):84–91.
59. Heinz SA, Henson DA, Austin MD, Jin F, Nieman DC (2010) Quercetin supplementation and upper respiratory tract infection: A randomized community clinical trial. *Pharmacol Res* 62(3):237–242.
60. Shan BE, Wang MX, Li RQ (2009) Quercetin inhibit human SW480 colon cancer growth in association with inhibition of cyclin D1 and survivin expression through Wnt/beta-catenin signaling pathway. *Cancer Invest* 27(6):604–612.
61. Lu SJ, et al. (2008) Biologic properties and enucleation of red blood cells from human embryonic stem cells. *Blood* 112(12):4475–4484.
62. Leung CG, et al. (2007) Requirements for survivin in terminal differentiation of erythroid cells and maintenance of hematopoietic stem and progenitor cells. *J Exp Med* 204(7):1603–1611.
63. Lee JS, et al. (2009) Senescent growth arrest in mesenchymal stem cells is bypassed by Wip1-mediated downregulation of intrinsic stress signaling pathways. *Stem Cells* 27 (8):1963–1975.
64. Park CH, et al. (2005) In vitro and in vivo analyses of human embryonic stem cell-derived dopamine neurons. *J Neurochem* 92(5):1265–1276.
65. Lee MY, et al. (2006) Local subplasma membrane Ca2+ signals detected by a tethered Ca2+ sensor. *Proc Natl Acad Sci USA* 103(35):13232–13237.
66. Vazquez-Martin A, et al. (2012) Metformin limits the tumourigenicity of iPS cells without affecting their pluripotency. *Scientific Reports* 2:964.
67. Ben-David U, et al. (2013) Selective elimination of human pluripotent stem cells by an oleate synthesis inhibitor discovered in a high-throughput screen. *Cell Stem Cell* 12(2): 167–179.